

On the magnetic field of the first Galactic ultraluminous X-ray pulsar Swift J0243.6+6124

Sergey S. Tsygankov,^{1,2*} Victor Doroshenko,³ Alexander A. Mushtukov,^{4,2}
Alexander A. Lutovinov² and Juri Poutanen^{1,2,5}

¹*Tuorla Observatory, Department of Physics and Astronomy, FI-20014 University of Turku, Finland*

²*Space Research Institute of the Russian Academy of Sciences, Profsoyuznaya str. 84/32, Moscow 117997, Russia*

³*Institut für Astronomie und Astrophysik, Universität Tübingen, Sand 1, D-72076 Tübingen, Germany*

⁴*Anton Pannekoek Institute of Astronomy, University of Amsterdam, Science Park 904, 1098 XH Amsterdam, The Netherlands*

⁵*Nordita, KTH Royal Institute of Technology and Stockholm University, Roslagstullsbacken 23, SE-10691 Stockholm, Sweden*

Accepted 2018 June 22. Received 2018 June 18; in original form 2018 April 22

ABSTRACT

We report on the monitoring of the final stage of the outburst from the first Galactic ultraluminous X-ray pulsar Swift J0243.6+6124, which reached ~ 40 Eddington luminosities. The main aim of the monitoring program with the *Swift*/XRT telescope was to measure the magnetic field of the neutron star using the luminosity of transition to the “propeller” state. The visibility constraints, unfortunately, did not permit us to observe the source down to the fluxes low enough to detect such a transition. The tight upper limit on the propeller luminosity $L_{\text{prop}} < 6.8 \times 10^{35} \text{ erg s}^{-1}$ implies the dipole component of the magnetic field $B < 10^{13} \text{ G}$. On the other hand, the observed evolution of the pulse profile and of the pulsed fraction with flux points to a change of the emission region geometry at the critical luminosity $L_{\text{crit}} \sim 3 \times 10^{38} \text{ erg s}^{-1}$ both in the rising and declining parts of the outburst. We associate the observed change with the onset of the accretion column, which allows us to get an independent estimate of the magnetic field strength close to the neutron stars surface of $B > 10^{13} \text{ G}$. Given the existing uncertainty in the effective magnetosphere size, we conclude that both estimates are marginally compatible with each other.

Key words: accretion, accretion discs – pulsars: general – stars: magnetic field – stars: neutron – X-rays: binaries – pulsars: individual: Swift J0243.6+6124

1 INTRODUCTION

The transient X-ray pulsar Swift J0243.6+6124 was discovered by the *Swift*/XRT telescope (Kennea et al. 2017) after an alert generated by the MAXI monitor on 2017 September 29 (Sugita et al. 2017). Spin period of the neutron star (NS) was measured at 9.68 s (Kennea et al. 2017; Jenke & Wilson-Hodge 2017). Analysis of the observed spin frequency changes allowed also to determine orbital parameters of the system using the *Fermi*/GBM data, which revealed a low-eccentric orbit ($e \sim 0.1$) with period $\sim 28 \text{ d}$ (Doroshenko et al. 2018; Jenke et al. 2018).

Based on the optical spectroscopic observations, Kouroubatzakis et al. (2017) suggested that optical counterpart in the system is late Oe- or early Be-type star. The Be/X-ray binary (BeXRB) nature of the source was later confirmed by Bikmaev et al. (2017). With peak flux reaching $F_{\text{peak}} \sim 7 \times 10^{-7} \text{ erg s}^{-1} \text{ cm}^{-2}$ in the outburst maximum, the

source represents one of the brightest X-ray sources and the brightest BeXRB ever observed. The distance to the source was independently estimated using the X-ray and optical observations. Optical photometry and spectroscopy obtained from the RTT-150 and BTA telescopes allowed to estimate the mass $M_{\text{opt}} = 16 \pm 2 M_{\odot}$ and radius $R_{\text{opt}} = 7 \pm 2 R_{\odot}$ of the Be counterpart, which implies the distance to the source of about 2.5 kpc (Bikmaev et al. 2017). On the other hand, analysis of the pulsars spin-up rate as a function of luminosity performed by Doroshenko et al. (2018) implies a lower limit on distance of $\sim 5 \text{ kpc}$. This disagreement was finally resolved by the *Gaia* observatory measured distance to the system of $d = 7.3^{+1.5}_{-1.2} \text{ kpc}$ ¹ (van den Eijnden et al., in prep.). Such a distance implies peak luminosity of up to $\sim 5 \times 10^{39} \text{ erg s}^{-1}$, exceeding the Eddington limit for a NS by

¹ obtained as a median value, assuming the priors recommended by the *Gaia* team, with the errors given at 16th and 84th percentile

* E-mail: sergey.tsygankov@utu.fi; juri.poutanen@utu.fi

a factor of 40. Thus, Swift J0243.6+6124 can be considered as the first Galactic X-ray pulsar, belonging to the recently discovered family of ultraluminous X-ray pulsars (see e.g., Bachetti et al. 2014; Fürst et al. 2016; Israel et al. 2017b,a; Tsygankov et al. 2017a). It is worth mentioning that here and below we refer to isotropic luminosity. Although some beaming of emission can be expected in the case of XRP, we argue that for Swift J0243.6+6124 it is negligible. It follows from the smoothness of the source lightcurve, which does not show any features even when the pulse profile changes significantly, i.e. when the critical and the Eddington luminosities are passed and the beaming pattern is changed (see below).

Swift J0243.6+6124 was observed with the *NuSTAR* observatory several times throughout the outburst. Preliminary results of the X-ray broadband spectroscopy demonstrate the presence of a high-temperature black body component ($kT \sim 3$ keV) in addition to the typical for X-ray pulsars cut-off power-law with photon index of ~ 1 and $E_{\text{cut}} \sim 20$ keV (Bahramian et al. 2017; Jaisawal et al. 2018). The X-ray spectrum of the source revealed no evidence for additional absorption features which could be associated with the cyclotron resonant scattering and provide an estimate of the magnetic field of the NS (for a review see e.g., Walter et al. 2015).

Knowledge of the magnetic field is essential for understanding physical processes responsible for the observed behaviour of X-ray pulsars, such as their extreme luminosities, significantly exceeding Eddington limit (Mushtukov et al. 2015b). The magnetic field strength in Swift J0243.6+6124 was estimated based on the observed spin-up rate of the pulsar and points to above-average value of $B \sim 10^{13}$ G (Doroshenko et al. 2018) under assumption that the source is located at distance ~ 6.6 kpc. While this estimate is in line with non-detection of the cyclotron absorption line in the wide energy range 0.3–80 keV, it is not model independent and thus requires verification.

Here we attempt to independently estimate the magnetic field of the NS based on observation of the transition of the source to the so called “propeller regime” when the accretion is centrifugally inhibited by the rotating magnetic field lines (Illarionov & Sunyaev 1975). This method was already verified in a very broad range of magnetic field strengths using a sample of magnetized NSs, consisting of accreting millisecond pulsar, classical X-ray pulsars and even pulsating ultra-luminous X-ray source (Tsygankov et al. 2016a,b; Lutovinov et al. 2017). In the case of Swift J0243.6+6124 its relative proximity and very good coverage of the tail of the outburst with the *Swift*/XRT telescope allowed us to monitor the source down to very low luminosities and to put an upper limit on the dipole component of the NS magnetic field in the system. Unfortunately, continuation of the monitoring until an actual transition to the propeller regime was impossible due to the Sun constraints of the visibility.

2 DATA ANALYSIS

We mostly rely on the data obtained with the XRT telescope (Burrows et al. 2005) onboard the *Neil Gehrels Swift Observatory* (Gehrels et al. 2004) during the fading phase of the outburst. Depending on the source brightness the obser-

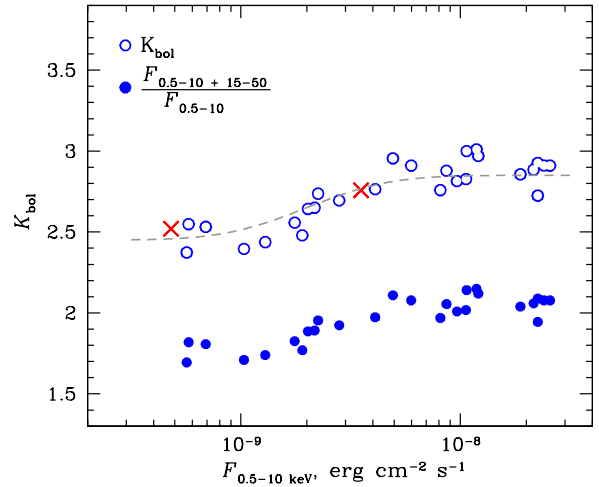


Figure 1. Dependence of the bolometric correction factor K_{bol} on the observed source flux in the 0.5–10 keV band (open circles), obtained after MJD 58110. Filled circles show the ratio of the total flux in the 0.5–10 keV plus 15–50 keV energy bands to the 0.5–10 keV flux as a function of the 0.5–10 keV flux. Red crosses show the K_{bol} values obtained from the broad-band spectra collected with the *NuSTAR* observatory. Grey dashed line shows the best fit to the K_{bol} values with the Gauss error function.

vations were performed both in Windowed Timing (WT) and Photon Counting (PC) modes. The data reduction, i.e. spectrum extraction, was done using the online tools (Evans et al. 2009)² provided by the UK Swift Science Data Centre. Only zero grade (single pixel) events were included into the product.

The source flux in each observation was determined based on the results of spectral fitting in the XSPEC package assuming the absorbed power-law model. Taking into account the low counting statistics in the very end of the outburst, we binned the spectra to have at least 1 count per energy bin and fitted them using W-statistic (Wachter et al. 1979).³ Given the known calibration uncertainties at low energies,⁴ we restricted our spectral analysis of the WT data to the 0.8–10 keV band and 0.3–10 keV in the PC data. In our spectral analysis we avoided usage of the *Swift*/XRT data for fluxes above $\sim 10^{-8}$ erg s⁻¹ cm⁻² strongly affected by the pile-up. Therefore our dataset starts from MJD 58110. This restriction does not affect any of our conclusions as only the final phase of the outburst is relevant for detection of the transition to the propeller regime.

To estimate the source luminosity and the mass accretion rate, and thus the magnetospheric radius of Swift J0243.6+6124 (see below), a reliable estimate of the bolometric flux is required. We estimate it based on the observed *Swift*/XRT fluxes following the procedure described in Tsygankov et al. (2017a). The observed spectra of X-ray pulsars are known to change with luminosity, so the bolometric correction is also luminosity dependent. To account

² http://www.swift.ac.uk/user_objects/

³ see XSPEC manual; <https://heasarc.gsfc.nasa.gov/xanadu/xspec/manual/XSappendixStatistics.html>

⁴ http://www.swift.ac.uk/analysis/xrt/digest_cal.php

for that we used the ratio of the total source flux in the 0.5–10 keV (from *Swift*/XRT data) plus 15–50 keV (from *Swift*/BAT) energy bands to the source flux in the 0.5–10 keV energy band to estimate the bolometric correction factor throughout the decay phase of the outburst.

The observed dependence of this ratio on flux in the 0.5–10 keV band is shown with filled blue points in Fig. 1. To relate the observed flux ratio and the actual bolometric correction factor K_{bol} we used the broadband observations performed with the *NuSTAR* observatory (marked by red crosses). The final bolometric correction factor values are shown with the open circles in the same figure, and are consistent with bolometric flux estimate by Doroshenko et al. (2018) using the *NuSTAR*, *Swift*/BAT and MAXI data at the higher end of fluxes considered here. In order to get a simple recipe for conversion of the observed *Swift*/XRT flux to the bolometric one we approximated the observed dependence of the correction factor on the observed flux in the 0.5–10 keV band with the Gauss error function, shown with the grey line. In the following analysis we apply this correction to all observational data and refer to the bolometrically corrected fluxes and luminosities unless stated otherwise. As can be seen from Fig. 1, the bolometric correction remains almost constant for low luminosities, so our results are essentially unaffected by the uncertainties in its reconstruction.

3 RESULTS

The bolometric and absorption corrected light curve of Swift J0243.6+6124 during the fading tail of the outburst is shown in the top panel of Fig. 2. A more or less gradual decrease of the flux is observed until around MJD 58207 when it reached the minimal value of $F_{\text{min}} \simeq 1.1 \times 10^{-10} \text{ erg s}^{-1} \text{ cm}^{-2}$. After this point the source started to rebrighten (Ruoco Escorial et al. 2018), which was followed again by a gradual decay. Another minimum with the same flux level has been reached around MJD 58235, again followed by the rebrightening. This temporary flux increases did not allow us to detect deeper minimum before the visibility was constrained by Sun. Such rebrightenings during the fading phase of giant outbursts in Be/X-ray pulsars systems were already reported by Tsygankov et al. (2017a) for SMC X-3.

The spectra of the source in the energy range covered by the XRT telescope were fitted using the absorbed power law model (PHABS*POWERLAW in the XSPEC package). The best-fit parameters demonstrate some moderate variability with the photon index being in the range of 0.8–1.3. The evolution of the photon index with time is shown in the middle panel of Fig. 2. Independently of the flux level the spectra demonstrated moderate hydrogen column density $N_{\text{H}} \simeq (0.8 - 1.0) \times 10^{22} \text{ cm}^{-2}$ (see bottom panel of Fig. 2) comparable to the interstellar absorption in the direction to the source, $N_{\text{H}} \simeq 0.9 \times 10^{22} \text{ cm}^{-2}$ (Willingale et al. 2013).

In order to probe changes in the geometrical and physical conditions in the emitting regions in the vicinity of the NS, we studied also the pulse profile evolution with the source intensity. As a result, a drastic change of the pulse profile shape in the 0.5–10 keV energy band was discovered around MJD 58100–58120 (see Fig. 3). In particular, the pulse profile at high fluxes is double-peaked with nearly equal intensity of both peaks, whereas at lower fluxes

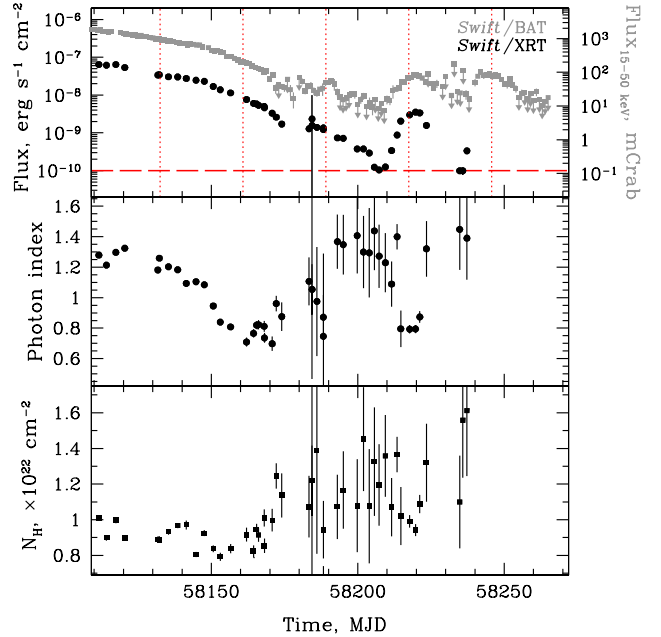


Figure 2. *Top:* The bolometrically corrected light curve of Swift J0243.6+6124 based on the *Swift*/XRT telescope data (black circles; left axis). Vertical red dotted lines represent moments of the periastron passage (Doroshenko et al. 2018). Horizontal dashed line shows the upper limit on the threshold flux for the propeller effect onset. Grey squares show evolution of hard X-ray flux in the 15–50 energy range from *Swift*/BAT (right axis). Arrows correspond to the 2σ upper limits. *Middle:* The evolution of the spectral photon index with time. *Bottom:* The evolution of the hydrogen column density N_{H} with time.

the profile has a single peak structure. Similar changes occurred also during the rising part of the outburst (around MJD 58040). Significant modifications of the pulse profile shape is accompanied also by the variations of the pulsed fraction. The pulsed fraction⁵ as a function of time is shown in Fig. 3. Note the strong changes on MJD 58040–58055 and MJD 58090–58120. At higher energies the observational coverage is limited, however, the source seems to exhibit similar behaviour of the pulse profile and pulsed fraction also in the hard band. Pulsed fraction variations along the outburst can be traced in this case based on the comparison of the pulsed flux measured by *Fermi*/GBM in the 15–50 keV energy band and the total *Swift*/BAT flux measured in the same energy band. As illustrated in Fig. 3, the pulsed flux fraction indeed increases at high fluxes similarly to the pulsed fraction measured directly by XRT. For the distance to the source of 7.3 kpc the transition luminosity can be estimated to be about $3 \times 10^{38} \text{ erg s}^{-1}$. It is important to emphasize that this change is not associated with the transition to the propeller regime and occurs at much higher luminosities. However, as we discuss below, it might also be relevant for the magnetic field strength estimation.

We were unable to obtain a robust phase coherent timing solution covering the entire outburst due to rapid change

⁵ It was calculated as $\text{PF} = (F_{\text{max}} - F_{\text{min}}) / (F_{\text{max}} + F_{\text{min}})$, where F_{max} and F_{min} are the maximum and minimum flux in the pulse profile, respectively.

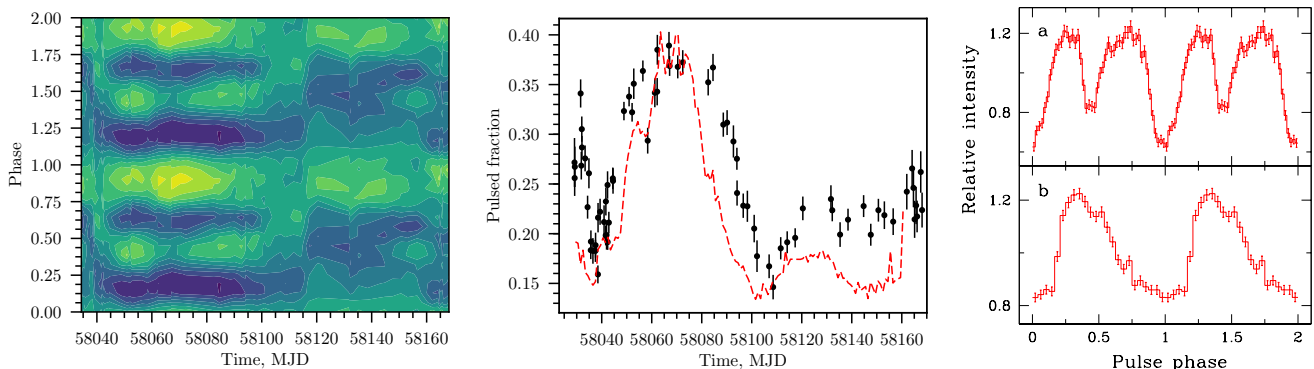


Figure 3. *Left:* Evolution of the pulse profile of the source throughout the outburst as observed by *Swift*/XRT in 0.8–10 keV energy range. Slices along the ordinate give normalized intensity as function of pulse phase at a given time. Pulse profiles were roughly aligned to minimize the offset between pairs of consequent pulse profiles. *Middle:* Observed pulsed fraction from the *Swift*/XRT data as function of time (black points). Ratio of pulsed flux measured by *Fermi*/GBM and total *Swift*/BAT flux, which gives indirect estimate of the pulsed fraction in hard 15–50 keV band is also shown (red line, arbitrarily scaled). *Right:* Observed pulse profile shape in 0.8–10 keV band before (a) and after (b) transition around MJD 58110.

of the short spin period and pulse profile shape, comparatively large gaps between XRT pointings, and remaining uncertainties in the orbital parameters. Therefore, we refrain from any conclusions regarding the specific phase shifts between different observations, however, strong changes of the observed pulse profile shape are apparent. To illustrate the pulse profile evolution we show also two profiles well before (MJD 58090) and after (MJD 58138) the transition in Fig. 3. This transition is discussed in more detail in Section 4.

4 DISCUSSION

Main goal of the work is to independently constrain the magnetic field of the NS in *Swift* J0243.6+6124 using the propeller effect. The propeller luminosity L_{prop} is defined by the equality of the magnetospheric radius (R_m) to the co-rotation radius (R_c). Under the assumption of the Keplerian motion in the accretion disc, matter can penetrate the magnetosphere and be accreted to the NS only if $R_m < R_c$ (Illarionov & Sunyaev 1975). In the opposite case centrifugal barrier stops the accretion and abrupt drop of the source luminosity should be observed.

The magnetospheric radius depends on the mass accretion rate and magnetic field strength, so a simple equation linking the limiting luminosity L_{prop} to the fundamental parameters of the NS can be derived by equating the co-rotation and magnetospheric radii (see, e.g. Campana et al. 2002)

$$L_{\text{prop}}(R) \simeq \frac{GMM_{\text{lim}}}{R} \simeq 4 \times 10^{37} k^{7/2} B_{12}^2 P^{-7/3} M_{1.4}^{-2/3} R_6^5 \text{ erg s}^{-1}, \quad (1)$$

where R_6 and $M_{1.4}$ are the NS radius and mass in units of 10^6 cm and $1.4M_\odot$, respectively, B_{12} is the magnetic field strength at the surface of the NS in units of 10^{12} G, P is the pulsar rotational period in seconds. Factor k is required to take into account difference of the magnetospheric radius in the case of disc accretion and classical Alfvén radius ($R_m = k \times R_A$) and is usually assumed to be $k = 0.5$ (Ghosh & Lamb 1978). It was recently shown

by Tsygankov et al. (2017b) that transition to the propeller regime is possible only for pulsars with relatively short pulse periods. From this point of view *Swift* J0243.6+6124, possessing the period of ~ 9.7 s, is a very good case study to make another step towards the verification of theory of accretion from the “cold disc” (Tsygankov et al. 2017b).

As can be seen from Fig. 2 no evidence of transition of the source to the propeller regime was observed. The lowest flux level detected by the XRT telescope before *Swift* J0243.6+6124 entered the rebrightening phase is $F_{\text{min}} \simeq 1.1 \times 10^{-10} \text{ erg s}^{-1} \text{ cm}^{-2}$.

Using this value as an upper limit for the threshold flux F_{prop} it is possible to derive an upper limit for the magnetic field strength. For the distance of $d = 7.3$ kpc and the coefficient $k = 0.5$, the propeller luminosity is $L_{\text{prop}} < 6.8 \times 10^{35} \text{ erg s}^{-1}$ and corresponding magnetic field $B < 6.2 \times 10^{12}$ G. This value is factor of two lower than the value derived from the analysis of spin period derivative (Doroshenko et al. 2018). However, given the strong dependence of the result on the assumed torque model and accretion disc effective radius, we consider agreement satisfactory. In particular, it is sufficient to assume $k \sim 0.35$ (see e.g., Chashkina et al. 2017) to increase the upper limit obtained from non-detection of the transition to the propeller at 10^{13} G, making it consistent with the accretion torque estimate. Note, however, that improvement on the upper limit on the propeller luminosity would deteriorate this agreement and thus imply presence of an appreciable non-dipole component of the field.

Additional information about the magnetic field strength can be obtained from the analysis of the pulse profile variations with luminosity. The sharp variations of a beam pattern with accretion luminosity can be caused by the transition from the sub-critical regime of accretion to the super-critical regime, when the radiation pressure becomes high enough to stop matter above the NS surface (Basko & Sunyaev 1976; Becker et al. 2012; Mushtukov et al. 2015a). In this case, rather small variations of the mass accretion rate can result in appreciable changes of the geometry of the emitting region and mod-

ification of the observed pulse profile and pulsed fraction (Gnedin & Sunyaev 1973).

The critical luminosity value L_{crit} depends on the magnetic field strength at the NS surface (Becker et al. 2012; Mushtukov et al. 2015a). For a “standard” magnetic field $B \sim 10^{12}$ G it is estimated at $L_{\text{crit}} \sim 10^{37}$ erg s $^{-1}$, and increases for stronger magnetic fields. If the observed variations of the pulse profile and pulsed fraction in Swift J0243.6+6124 are caused by the transition through the critical luminosity, it points to the magnetic field of the order of $\gtrsim 10^{13}$ G at the surface. This value is, again, marginally compatible with the other estimates. We emphasize, however, that the transition to the propeller was actually not observed, so the transition flux can be, in principle, significantly lower, which would make the two estimates inconsistent with each other. As discussed in Tsygankov et al. (2017a), this discrepancy can, however, still be resolved assuming that the magnetic field of the NS has non-negligible multipole component. It also indicates that local X-ray radiation is dominated by extraordinary mode of polarization characterized by a lower cross-section of interaction with the accreting material (Harding & Lai 2006; Mushtukov et al. 2016). We emphasize that to explore this possibility it is important to continue monitoring of the source shall it enter another outburst.

5 CONCLUSIONS

Here we presented the results of the monitoring of the newly discovered unique X-ray pulsar Swift J0243.6+6124 with the *Swift*/XRT telescope in the tail of its giant outburst. The source in fact is the brightest BeXRP in the Milky Way and belongs to the recently discovered family of ultraluminous X-ray pulsars. The main goal of the observational campaign was to detect the transition of the pulsar to the “propeller” state and, hence, to estimate the dipole component of the magnetic field of the NS powering this source. Unfortunately, the visibility constraints did not permit us to observe the source down to the fluxes low enough to detect such a transition. However, we were able to put a tight upper limit on the propeller luminosity $L_{\text{prop}} < 6.8 \times 10^{35}$ erg s $^{-1}$, and, correspondingly, an upper limit on the dipole component of the NS magnetic field strength $B \lesssim 10^{13}$ G. This value is in line with estimates obtained based on the observed spin-up rate of the pulsar, and possible transition of the pulsar through the critical luminosity at $L_{\text{crit}} \sim 3 \times 10^{38}$ erg s $^{-1}$ suggested by the observed drastic change of the pulse profile shape around MJD 58110. Swift J0243.6+6124 can serve as a unique Galactic laboratory for studying physics of ultraluminous X-ray pulsars over the large dynamic range of luminosities.

ACKNOWLEDGEMENTS

This work was supported by the Russian Science Foundation grant 14-12-01287 (SST, AAL, AAM). VD thank the Deutsches Zentrum für Luft- und Raumfahrt (DLR) and Deutsche Forschungsgemeinschaft (DFG) for financial support. We also express our thanks to the *Swift* ToO team for prompt scheduling and executing of our observations.

REFERENCES

- Bachetti M., et al., 2014, *Nature*, **514**, 202
 Bahramian A., Kennea J. A., Shaw A. W., 2017, The Astronomer’s Telegram, **10866**
 Basko M. M., Sunyaev R. A., 1976, *MNRAS*, **175**, 395
 Becker P. A., et al., 2012, *A&A*, **544**, A123
 Bikmaev I., et al., 2017, The Astronomer’s Telegram, **10968**
 Burrows D. N., et al., 2005, *Space Sci. Rev.*, **120**, 165
 Campana S., Stella L., Israel G. L., Moretti A., Parmar A. N., Orlandini M., 2002, *ApJ*, **580**, 389
 Chashkina A., Abolmasov P., Poutanen J., 2017, *MNRAS*, **470**, 2799
 Doroshenko V., Tsygankov S., Santangelo A., 2018, *A&A*, **613**, A19
 Evans P. A., et al., 2009, *MNRAS*, **397**, 1177
 Fürst F., et al., 2016, *ApJ*, **831**, L14
 Gehrels N., et al., 2004, *ApJ*, **611**, 1005
 Ghosh P., Lamb F. K., 1978, *ApJ*, **223**, L83
 Gnedin Y. N., Sunyaev R. A., 1973, *A&A*, **25**, 233
 Harding A. K., Lai D., 2006, *Reports on Progress in Physics*, **69**, 2631
 Illarionov A. F., Sunyaev R. A., 1975, *A&A*, **39**, 185
 Israel G. L., et al., 2017a, *Science*, **355**, 817
 Israel G. L., et al., 2017b, *MNRAS*, **466**, L48
 Jaisawal G. K., Naik S., Chenevez J., 2018, *MNRAS*, **474**, 4432
 Jenke P., Wilson-Hodge C. A., 2017, The Astronomer’s Telegram, **10812**
 Jenke P., Wilson-Hodge C. A., Malacaria C., 2018, The Astronomer’s Telegram, **11280**
 Kennea J. A., Lien A. Y., Krimm H. A., Cenko S. B., Siegel M. H., 2017, The Astronomer’s Telegram, **10809**
 Kouroubatzakis K., Reig P., Andrews J., A. Z., 2017, The Astronomer’s Telegram, **10822**
 Lutovinov A. A., Tsygankov S. S., Krivonos R. A., Molkov S. V., Poutanen J., 2017, *ApJ*, **834**, 209
 Mushtukov A. A., Suleimanov V. F., Tsygankov S. S., Poutanen J., 2015a, *MNRAS*, **447**, 1847
 Mushtukov A. A., Suleimanov V. F., Tsygankov S. S., Poutanen J., 2015b, *MNRAS*, **454**, 2539
 Mushtukov A. A., Nagirner D. I., Poutanen J., 2016, *Phys. Rev. D*, **93**, 105003
 Ruoco Escorial A., Degenaar N., van den Eijnden J., Wijnands R., 2018, The Astronomer’s Telegram, **11517**
 Sugita S., et al., 2017, The Astronomer’s Telegram, **10803**
 Tsygankov S. S., Mushtukov A. A., Suleimanov V. F., Poutanen J., 2016a, *MNRAS*, **457**, 1101
 Tsygankov S. S., Lutovinov A. A., Doroshenko V., Mushtukov A. A., Suleimanov V., Poutanen J., 2016b, *A&A*, **593**, A16
 Tsygankov S. S., Doroshenko V., Lutovinov A. A., Mushtukov A. A., Poutanen J., 2017a, *A&A*, **605**, A39
 Tsygankov S. S., Mushtukov A. A., Suleimanov V. F., Doroshenko V., Abolmasov P. K., Lutovinov A. A., Poutanen J., 2017b, *A&A*, **608**, A17
 Wachter K., Leach R., Kellogg E., 1979, *ApJ*, **230**, 274
 Walter R., Lutovinov A. A., Bozzo E., Tsygankov S. S., 2015, *A&ARv*, **23**, 2
 Willingale R., Starling R. L. C., Beardmore A. P., Tanvir N. R., O’Brien P. T., 2013, *MNRAS*, **431**, 394

This paper has been typeset from a \LaTeX file prepared by the author.